Processing and Application of Ceramics 13 [2] (2019) 124–131
https://doi.org/10.2298/PAC1902124K

Mechanical properties and band structure of CdSe and CdTe nanostructures at high pressure – A first-principles study

Natarajan Kishore[1], Veerappan Nagarajan[2], Ramanathan Chandiramouli[2,*]

[1]*School of Mechanical Engineering, SASTRA Deemed University, Tirumalaisamudram, Thanjavur 613 401, India*
[2]*School of Electrical & Electronics Engineering, SASTRA Deemed University, Tirumalaisamudram, Thanjavur 613 401, India*

Received 21 August 2018; Received in revised form 29 January 2019; Accepted 31 March 2019

Abstract

First-principles calculations for CdSe and CdTe nanostructures were carried out to study their mechanical properties and band structure under the uniaxial pressure range of 0 to 50 GPa. It was presumed that the CdSe and CdTe nanostructures exist in the zinc-blende phase under high pressure. The mechanical properties, such as elastic constants, bulk modulus, shear modulus and Young's modulus, were explored. Furthermore, Cauchy pressure, Poisson's ratio and Pugh's criterion were studied under high pressure for both CdSe and CdTe nanostructures, and the results show that they exhibit ductile property. The band structure studies of CdSe and CdTe were also investigated. The findings show that the mechanical properties and the band structures of CdSe and CdTe can be tailored with high pressure.

Keywords: *CdSe, CdTe, high pressure, band structure, elastic constant*

I. Introduction

The metal chalcogenide compounds such as CdTe and CdSe are currently under extensive research owing to their wide application in optoelectronics and electronic devices [1]. Moreover, the tunable electronic properties of CdTe and CdSe find their way to various applications due to their fascinating properties, such as direct and wide band gap, high absorption coefficient etc. [2]. Benkhettou *et al.* [3] studied the structural properties and high-pressure stability of CdS and CdSe. Furthermore, for CsCl type structure of CdSe, the thermodynamic stability ranges were evaluated and the structural properties of different phases are presented. Zakharov *et al.* [4] estimated the structural and electronic properties of CdSe under high pressure and the findings show that CdSe exhibits CsCl type structure under high pressure. Tolbert *et al.* [5] explored the stability of CdSe nanocrystal under high pressure derived from both kinetics of the transformation and thermodynamics, which are substantially dissimilar in its finite size. Besides, the theoretical and experimental band structures of CdS and CdSe under high pressure were determined by Cervantes *et al.* [6]. Kong group [7] investigated the crystal structure and structural phase transitions for CdSe under high pressure. Additionally, the conversion of spheroidal shaped arrays of CdSe nanocrystal into 1D luminescent nanowire under high pressure was reported by Li and coworkers [8]. Matsuishi [9] investigated the structural and optical properties of CdSe nanostructure by fabricating both nanoparticles and nanosheets using organic molecules as a template. Jacobs *et al.* [10] demonstrated that at ambient pressure, metastable CdSe nanocrystals exist depending on the physical size of the particle. Structural transformation of CdSe nanorods under pressure was investigated by Lee *et al.* [11]. Grant *et al.* [12] studied the photoluminescence property of pressure-induced CdSe quantum dot solids. Aliyu *et al.* [13] reported about the application of CdTe in solar cells and the strategies to overcome the shortcoming of CdTe in this technology. Seetawan *et al.* [14] studied the mechanical properties of CdTe semiconductors with the rock salt structure in a temperature range of 300–700 K. Martínez *et al.* [15] investigated the mechanical properties of CdTe alloyed with 2 and 5 at.% of Zn using density functional theory. The crystal

*Corresponding author: tel: +91 948 9566466,
e-mail: *rcmoulii@gmail.com*

structure of CdSe and CdTe exists in different types such as rock salt, zinc-blende and wurtzite and these are determined by their degrees of metallic bond, covalent and ionic bond. Typically, II-VI semiconductors undergo the pressure-induced transition from zinc-blende (ZB) towards rock salt (RS) after which β-Sn type phases are obtained [16].

In the present framework, we investigate CdSe and CdTe nanostructures in the zinc-blende structure in the uniaxial pressure range from 0 to 50 GPa. It is well known that zinc-blende structure is the natural phase of CdTe, whereas apart from cubic CdSe, it also exists in the wurtzite structure. Besides, it was confirmed that thin crystals of CdSe with the zinc-blende phase can be prepared by molecular beam epitaxy technique [17,18]. Although, the pressure induced elastic constants of CdSe up to 30 GPa were already reported [2], the band structure and the mechanical properties of pressure-induced CdSe and CdTe nanostructures in the zinc-blende phase have not been explored. Thus, our goal is to present a systematic study on the mechanical properties and the band structures of zinc blende CdSe and CdTe nanostructures under high pressure by using the first-principles study.

II. Computational details

We employed density functional theory (DFT) through SIESTA package [19] to perform the first-principles calculations on CdSe and CdTe nanostructures. The Perdew-Burke-Ernzerhof (PBE) exchange-correlation functional within the framework of generalized gradient approximation (GGA) was used to perform local structural relaxation, which was implemented with SIESTA package [20,21]. To explore these nanostructures, GGA/PBE functional remains the most relevant one to perform the first-principles calculation. The grid-mesh cut-off was adjusted to be 400 eV, and we performed full structural relaxation with conjugate gradient algorithm through double-zeta-polarization (DZP) basis set [22,23] until the Hellmann-Feynman force was met to 0.02 eV/Å. Besides, by employing SIESTA code, the band structures and mechanical properties of CdSe and CdTe were determined with the Brillouin zones fragmented with $8 \times 8 \times 8$ k points using Monkhorst-pack.

III. Results and discussion

3.1. Elastic constants

The examination of the elastic properties is crucial to understand the chemical bonds, electronic and mechanical properties and mechanical stability of materials [24]. To inspect an assortment of crucial solid-state phenomena such as stability, ductility, brittleness and anisotropy of CdSe and CdTe nanostructures, exploration of elastic constants is essential to demonstrate its pressure-induced mechanical properties. Figure 1 depicts the cubic nanostructures of CdSe and CdTe. For a cubic structure, there are three separate elastic constants namely C_{11}, C_{12}, and C_{44} that can be determined through the lattice deformation as reported by Deligoz *et al.* [2]. The authors have successfully studied the electronic, elastic and lattice dynamical properties of cadmium chalcogenides using DFT studies. Based on the above report, we have calculated all three elastic constants for CdSe and CdTe cubic systems.

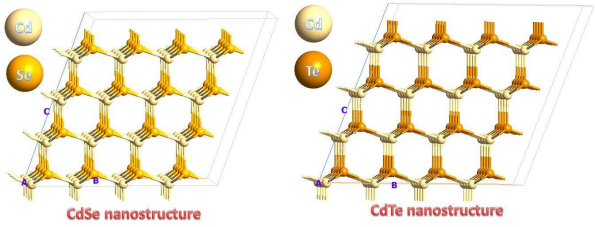

Figure 1. Schematic diagram of cubic CdSe and CdTe nanostructures

Initially, we perceived the elementary condition for the cubic structure as given in Jamal *et al.* [25]. Besides, for the cubic structure, it is anticipated that the Born stability criteria are contented:

$$C_{11} - C_{12} > 0,\ C_{11} + 2C_{12} > 0,\ C_{44} > 0$$

From Table 1, it is evident that both CdSe and CdTe nanostructures are mechanically stable as the Born stability criteria are fulfilled. Moreover, it is noticed that the obtained values are in compliance with the previously reported studies, thus ensuring the correctness of our calculations for different pressure values.

3.2. Mechanical properties

Mechanical properties of CdSe and CdTe are deciphered from the Voigt-Reuss-Hill (VRH) averaging schemes, respectively. The Reuss and Voigt bulk and shear modulus for the cubic system were given by the

Table 1. Pressure-induced elastic constants of cubic CdSe and CdTe nanostructures

Pressure [GPa]	C_{11}	C_{12}	C_{44}
CdSe			
0	87.80	36.92	35.96
10	121.95	46.70	46.84
20	214.49	100.13	82.00
30	366.55	185.78	138.91
40	485.57	257.44	187.76
50	602.11	328.48	231.42
CdTe			
0	63.39	32.42	23.52
10	96.78	49.63	31.52
20	229.03	126.19	77.89
30	339.54	192.06	118.91
40	435.07	251.95	150.41
50	515.10	304.19	174.52

following equations [26]:

$$B_V = B_H = \frac{C_{11} + 2C_{12}}{3} \quad (1)$$

$$G_V = \frac{C_{11} - C_{12} + 3C_{44}}{5} \quad (2)$$

$$G_R = \frac{5C_{44}(C_{11} - C_{12})}{4C_{44} + 3(C_{11} - C_{12})} \quad (3)$$

The Hill bulk and shear moduli are expressed as:

$$B_H = \frac{C_V + C_R}{2} \quad (4)$$

$$G_H = \frac{G_V + G_R}{2} \quad (5)$$

Poisson's ratio (ν) and Young's modulus (E) are resolved from the following relations:

$$E = \frac{9B \cdot G}{3B + G} \quad (6)$$

$$\nu = \frac{3B - 2G}{2(3B + G)} \quad (7)$$

Moreover, the pressure-induced measurement of the volume detention is established by bulk modulus (B), whereas the material's impedance to reversible deformation is given by shear modulus (G). The known fact is that stiffness of any material is a measure of the bulk modulus. Similarly, the hardness of any material complies with its shear modulus. Besides, the ductility is depicted by Young's modulus, which also yields stiffness measurements in solids [27]. The pressure-induced values for shear modulus, Young's modulus and bulk modulus of CdSe and CdTe nanostructures under the pressure of up to 50 GPa are represented in Table 2 and 3. It is ascertained that the magnitude of Young's modulus intensifies with the increase in pressure up to 50 GPa. It can also be witnessed that the stiffness follows correspondingly. Furthermore, up to 50 GPa, the upsurge in the resistance to volume deformation given by bulk modulus is observed. In addition, the shear modulus also amplifies with the increase in pressure. For CdSe, the trend in our calculated values up to 30 GPa is in good agreement with the reported data [2].

Now we will turn the discussion to anisotropic index, which is one of the important elastic properties for many applications [28]. The anisotropic percentage (A_B and A_G) and the universal anisotropic index (A^U) are given by the following equations:

$$A_B = \frac{B_V - B_R}{B_V + B_R} \quad (8)$$

$$A_G = \frac{G_V - G_R}{G_V + G_R} \quad (9)$$

$$A^U = \frac{5G_V}{G_R} + \frac{B_V}{B_R} - 6 \geq 0 \quad (10)$$

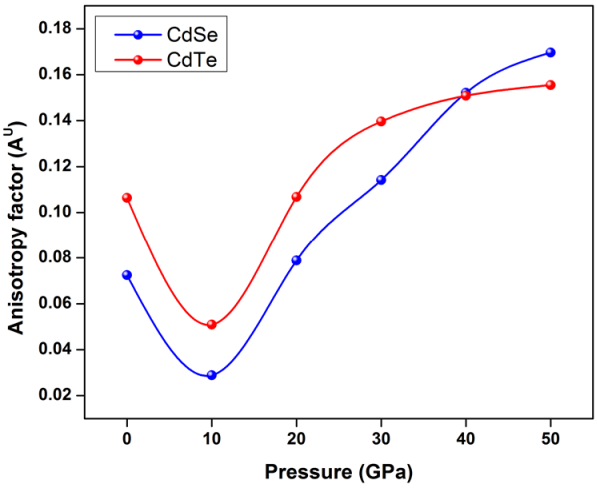

Figure 2. Uniaxial pressure versus universal anisotropy of CdSe and CdTe nanostructures

Table 2. Pressure-induced bulk modulus (B), shear modulus (G) and Young's modulus (E) of CdSe nanostructure in ZB phase

Unuaxial pressure [GPa]	B_R	B_V	B_H	G_R	G_V	G_H	E_R	E_V	E_H
0	53.89	53.89	53.89	30.86	31.75	31.31	65.95	65.95	65.95
10	71.78	71.78	71.78	42.66	43.16	42.91	96.09	96.09	96.09
20	138.25	138.25	138.25	69.87	72.08	70.97	150.76	150.76	150.76
30	246.66	246.87	246.77	114.78	119.98	117.38	241.08	242.48	244.26
40	333.49	333.49	333.49	149.20	158.28	153.74	307.17	307.17	307.17
50	419.69	419.69	419.69	181.28	193.57	187.42	370.21	370.21	370.21

Table 3. Pressure-induced bulk modulus (B), shear modulus (G) and Young's modulus (E) of CdTe nanostructure in ZB phase

Unuaxial pressure [GPa]	B_R	B_V	B_H	G_R	G_V	G_H	E_R	E_V	E_H
0	42.75	42.75	42.75	19.48	20.31	19.89	41.45	41.45	41.45
10	65.35	65.35	65.35	27.78	28.34	28.06	63.14	63.14	63.14
20	160.85	160.99	160.92	64.85	67.60	66.23	139.07	139.89	141.11
30	241.22	241.22	241.22	95.51	100.84	98.18	200.75	200.75	200.75
40	312.99	312.99	312.99	119.65	126.87	123.26	250.28	250.28	250.28
50	374.49	374.49	374.49	138.29	146.89	142.59	289.22	289.22	289.22

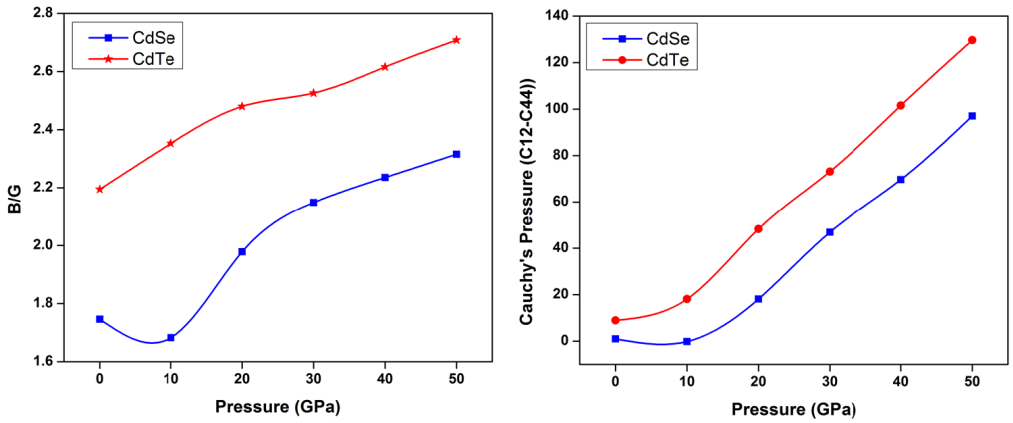

Figure 3. Cauchy's pressure versus uniaxial pressure (a) and Pugh's criterion versus uniaxial pressure (b) for CdSe and CdTe nanostructures

where B_R, B_V, G_V, G_R are the Reuss and Voigt bulk and shear moduli, respectively [29]. The divergence of A^U from zero represents the anisotropic property. The pressure-induced universal anisotropic index (A^U) of CdSe and CdTe nanostructures, depicted in Fig. 2, decreases initially from 0 to 10 GPa, and beyond 10 GPa A^U increases up to 50 GPa. The upsurge in A^U can be associated with the increase in pressure, leading to the distortion of lattice parameters, which in turn imputes to valence electrons being localized. It can be concluded that both CdSe and CdTe possess anisotropy property in the applied pressure range.

The Cauchy's pressure ($C_{12} - C_{44}$), Pugh's criterion (B/G ratio) and Poisson's ratio are necessary mechanical characteristics in order to distinguish brittleness and ductility. The ductile nature of the material is demonstrated by the positive magnitude of Cauchy's pressure [30], whereas a negative value signifies brittleness and nonmetallic in conjunction with directional bonding. From Fig. 3a it can be observed that the intensity of Cauchy's pressure increases with the induced pressure. Moreover, both CdSe and CdTe remain ductile in nature.

With respect to the Pugh's criterion, the material possesses brittleness, if B/G is smaller than 1.75; otherwise it is ductile in nature [31]. From Table 4 and Fig. 3b, it is observed that the ductility of CdTe upsurges monotonically with the increasing pressure. CdSe initially downturns and becomes brittle at 10 GPa after which the ductile nature intensifies with the escalating pressure. The resolution of bonding between materials and their plasticity is determined by Poisson's ratio. The value less than 0.1 suggests the brittle nature of the material, whereas Poisson's ratio greater than 0.26 demonstrates ductility [32]. For CdSe it is observed (Fig. 4 and Table 4) that, the Poisson's ratio decreases initially with an increase in pressure up to 10 GPa after which the value increases thereby up to 50 GPa. Besides, the Poisson's ratio for CdTe increases monotonically upon intensifying pressure. However, it can be noticed that both CdSe and CdTe exhibit ductility throughout the pressure range. The ductile nature of CdSe and CdTe nanostructures is governed by the fact that, the material undergoes significant plastic deformation as the valence electrons act as a lubricant throughout the pressure range.

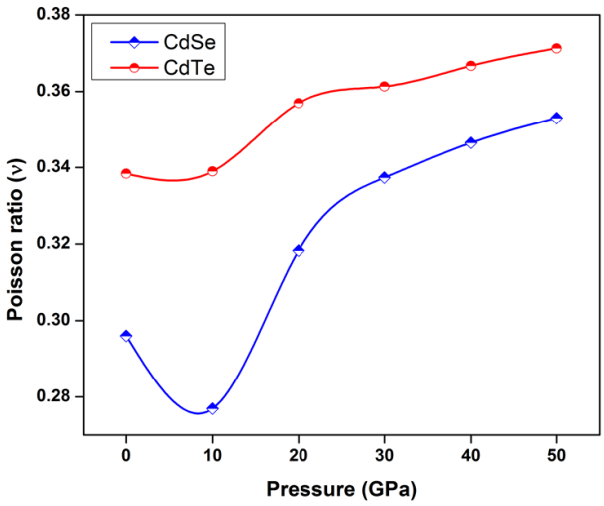

Figure 4. Uniaxial pressure versus Poisson's ratio for CdSe and CdTe nanostructures

Table 4. Pressure-induced Pugh's criterion, Poisson's ratio and hardness for CdSe and CdTe nanostructures

Uniaxial	Pugh's Criterion (B/G)		Poisson's Ratio (ν)		Hardness [GPa]	
pressure [GPa]	CdSe	CdTe	CdSe	CdTe	CdSe	CdTe
0	1.746	2.195	0.296	0.338	5.534	3.081
10	1.683	2.353	0.277	0.339	7.260	3.660
20	1.979	2.480	0.318	0.357	8.562	6.282
30	2.149	2.526	0.337	0.361	11.076	8.094
40	2.235	2.616	0.347	0.367	12.754	9.122
50	2.315	2.708	0.353	0.371	14.065	9.717

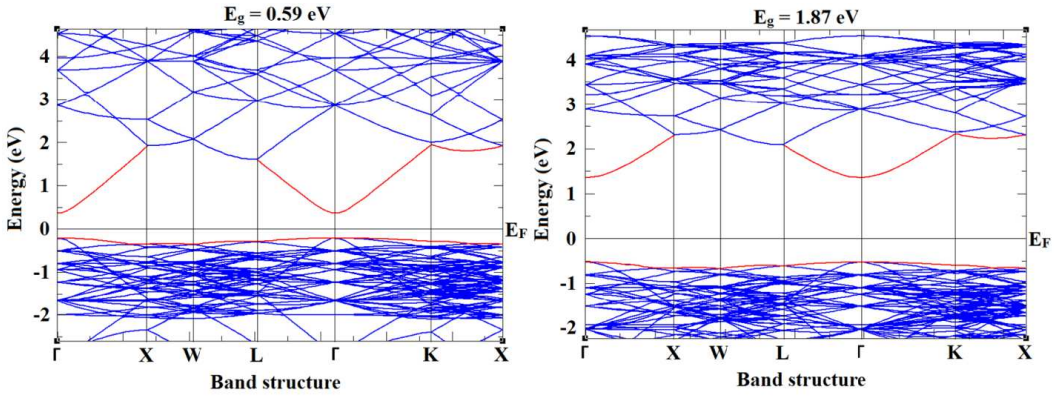

Figure 5. Energy band structure of CdSe and CdTe nanostructures at 0 GPa

The impedance against deformation is established by hardness H_V [33] expressed by the following equation where $K = G/B$ [29]:

$$H_V = 0.92K^{1.137}G^{0.708} \tag{11}$$

From Table 4, it can be concluded that the hardness intensifies with the increase in pressure for both CdSe and CdTe nanostructures, respectively. This increase is advocated due to the suppression of the motion of valence electrons, which in turn uplifts the stiffness or otherwise Young's modulus (as witnessed by previous results) of the material. Thus, the impedance against external force reveals the hardness in CdSe and CdTe nanostructures.

3.3. Band structures

A band gap of 0.59 eV was observed along the gamma point for CdSe nanostructure at 0 GPa (Fig. 5). Moreover, it is noticed that the band gap is found to be 1.87 eV for CdTe (Fig. 5). The raise in the band gap of CdTe with increasing pressure accounts to the formation of higher atomic number tellurium than cadmium. Furthermore, this band gap increase is accredited to the overlapping of [Kr] $4d^{10}\,5s^2$ in cadmium with the [Kr] $4d^{10}\,5s^2\,5p^4$ of tellurium. It is observed from Table 5, that the estimated band gap magnitude at 0 GPa complies with the previously reported theoretical and experimental results respectively [37,38].

In the case of CdSe, it is witnessed that by intensifying the pressure, the band gap increases to 1.13 eV

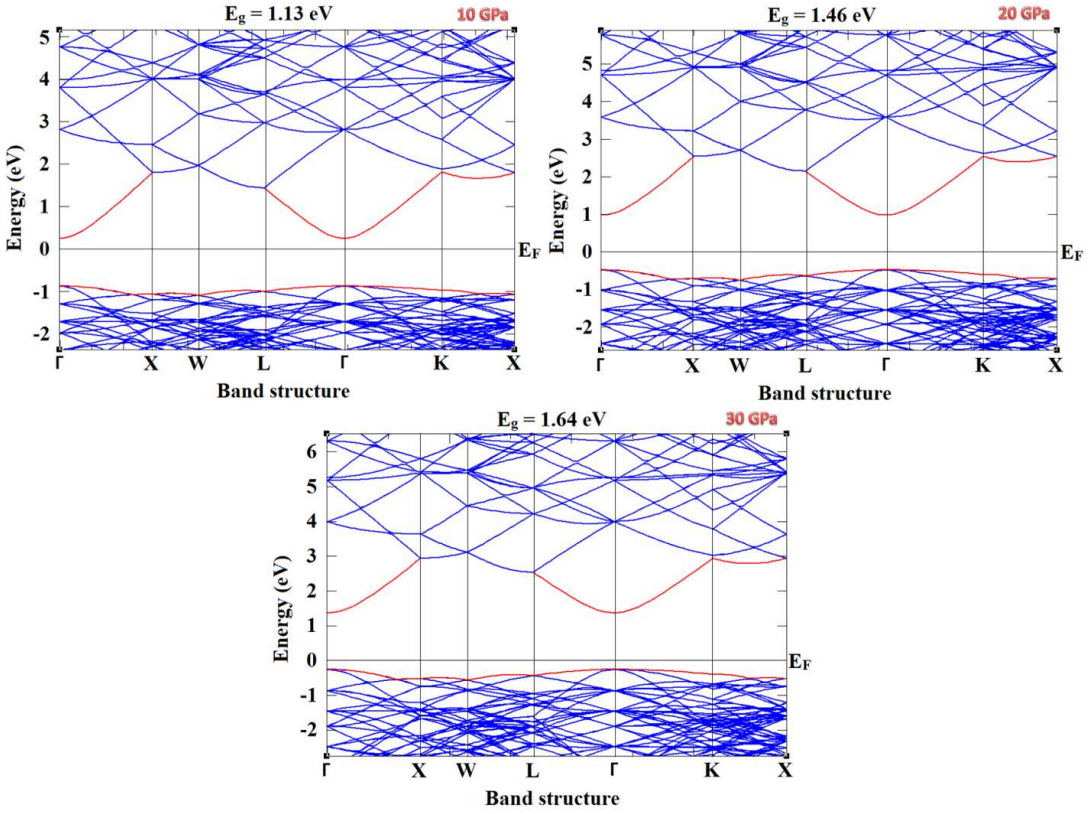

Figure 6. Energy band structure of CdSe nanostructure at 10, 20 and 30 GPa

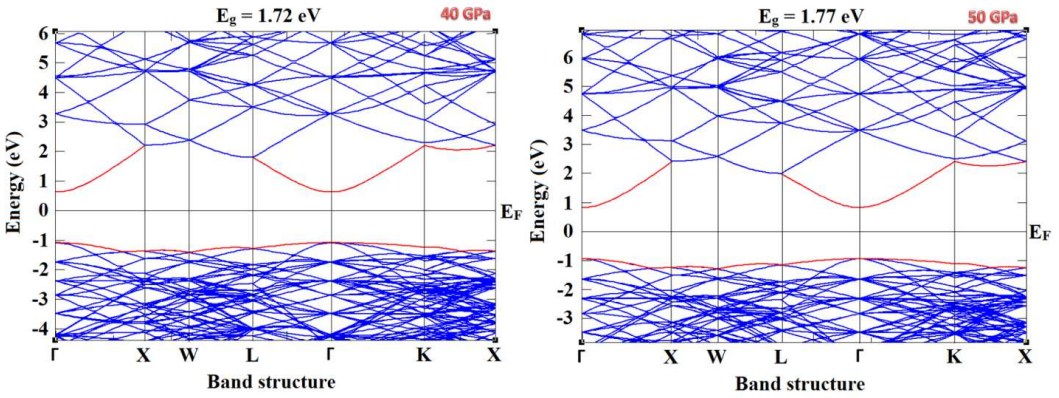

Figure 7. Energy band structure of CdSe nanostructure at 40 and 50 GPa

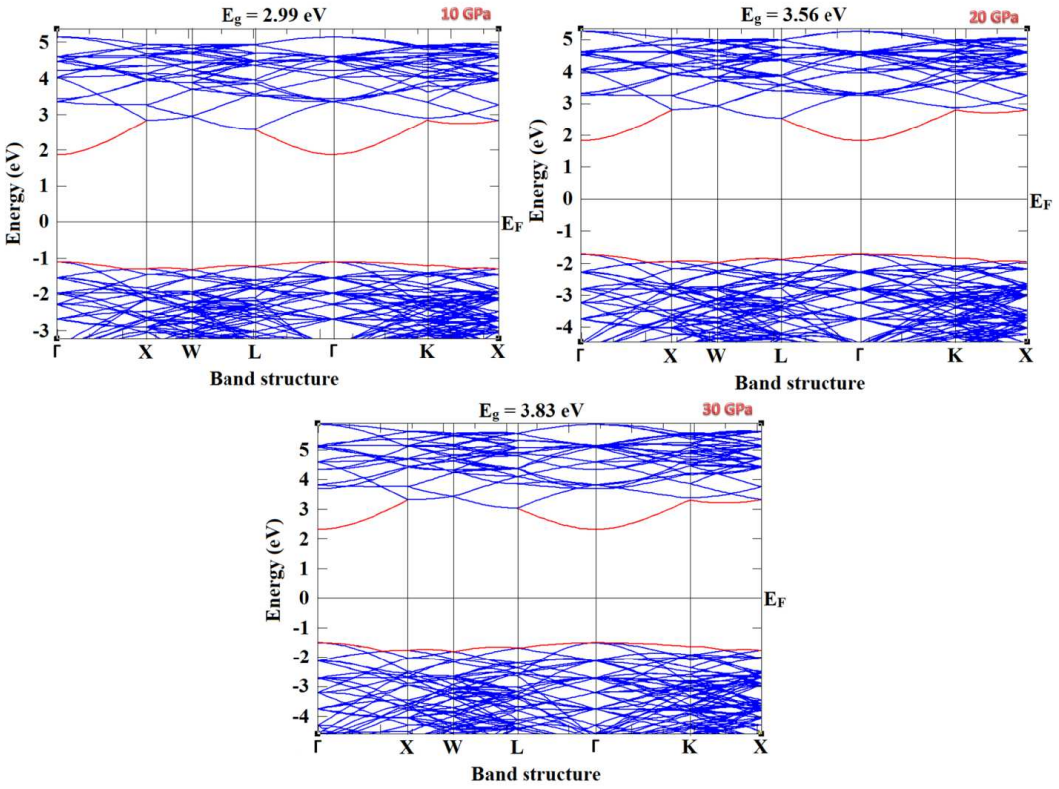

Figure 8. Energy band structure of CdTe nanostructure at 10, 20 and 30 GPa

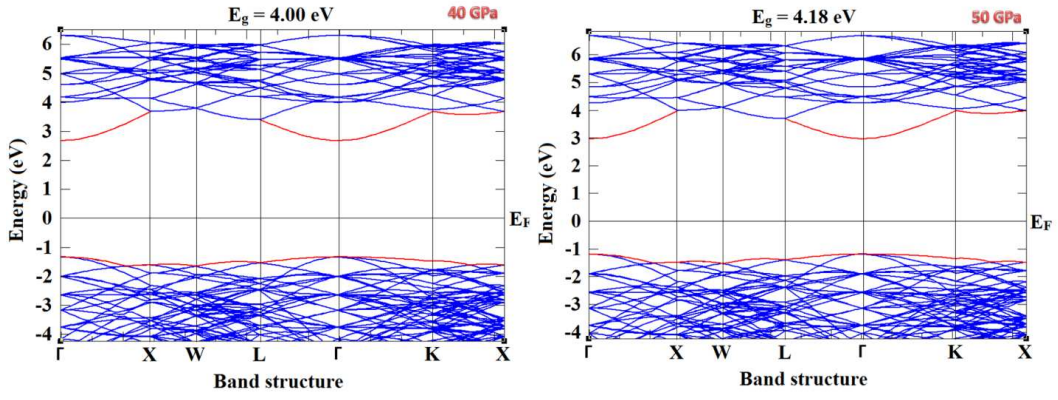

Figure 9. Energy band structure of CdTe nanostructure at 40 and 50 GPa

Table 5. The calculated energy direct band gap of CdSe and CdTe at 0 GPa along with the previously reported results

Nanostructure	Bandgap (at Γ) [eV]	Reference
CdSe	0.59	Present work
	0.76	[37]
CdTe	1.87	Present work
	1.76	[37]
	1.51	[38]

at pressure of 10 GPa and this increase continues to 1.77 eV until 50 GPa. The band structure of CdSe nanostructure in the uniaxial pressure, range from 0 to 50 GPa, is shown in Figs. 6 and 7. Concurrently, for CdTe nanostructure, the band gap is noticed to be 2.99 eV at 10 GPa and rises to 4.18 eV at 50 GPa, as shown in Figs. 8 and 9. The increase in the band gap can be associated with the decrease in interatomic distances when uniaxial pressure is enforced. The reason behind this is the pressure induced shrinking of lattice parameters as depicted in Fig. 10.

Moreover, declining unit cell volume and parameters, as shown in Figs. 10 and 11, are governed by the fact that the increase in the pressure leads to distorted lattice parameters, which shows a decreasing trend upon increase in the pressure. Besides, the motion of electrons also gets facilitated in CdSe and CdTe nanostructures owing to increase in the pressure that leads to the ductile nature of both CdSe and CdTe nanostructure under induced pressure.

IV. Conclusions

By the first-principles study, the mechanical properties and the band structure studies of the pressure induced CdSe and CdTe nanostructures were investigated. The elastic constants were determined to establish different moduli. Moreover, the elastic constants at 0 GPa are found to be analogous with the previously reported values, thus indicating the correctness of our calculations. Besides, bulk modulus, shear modulus and Young's modulus were found to increase monotonically with the increasing pressure. The anisotropy factor and hardness were also examined along with ductility. Moreover, the band gap of CdSe and CdTe was found to increase with the intensifying pressure. To our knowledge, the mechanical properties of CdSe and CdTe in ZB phase for the uniaxial pressure, range of 0 to 50 GPa, are reported for the first time. The findings suggest that the band gap and mechanical properties such as ductility can be fine-tuned upon the induced high pressure.

References

1. Y. Wang, "Luminescent CdTe and CdSe semiconductor nanocrystals: Preparation, optical properties and applications", *J. Nanosci. Nanotechnol.*, **8** [3] (2008) 1068–1091.
2. E.Ã. Deligoz, K. Colakoglu, Y. Ciftci, "Elastic, electronic, and lattice dynamical properties of CdS, CdSe, and CdTe", *Phys. B Condens. Matter*, **373** [1] (2006) 124–130.
3. N. Benkhettou, D. Rached, B. Soudini, M. Driz, "High-pressure stability and structural properties of CdS and CdSe", *Phys. Status Solidi Basic Res.*, **241** [1] (2004) 101–107.
4. O. Zakharov, A. Rubio, M.L. Cohen, "Calculated structural and electronic properties of CdSe under pressure", *Phys. Rev. B - Condens. Matter Mater. Phys.*, **51** [8] (1995) 4926–4930.
5. H. Tolbert, A.P. Alivisatos, "The wurtzite to rock salt structural transformation in CdSe nanocrystals under high pressure", *J. Chem. Phys.*, **102** [11] (1995) 4642–4656.
6. P. Cervantes, Q. Williams, M. Côté, O. Zakharov, M.L. Cohen, "Band structure of CdS and CdSe at high pressure", *Phys. Rev. B - Condens. Matter Mater. Phys.*, **54** [24] (1996) 17585–17590.
7. B. Kong, T.X. Zeng, Z.W. Zhou, D.L. Chen, X.W. Sun, "High pressure phase transitions for CdSe", *Bull. Mater. Sci.*, **37** [3] (2014) 549–552.
8. B. Li, K. Bian, X. Zhou, P. Lu, S. Liu, I. Brener, M. Sinclair, T. Luk, H. Schunk, L. Alarid, P.G. Clem, Z. Wang, H. Fan, "Pressure compression of CdSe nanoparticles into

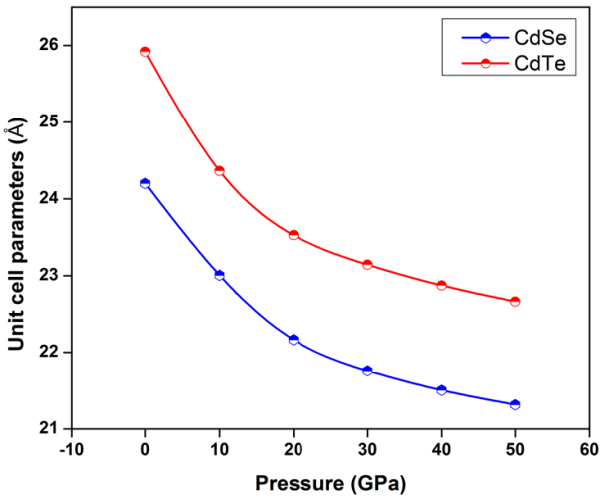

Figure 10. Unit cell parameters against uniaxial pressure for CdSe and CdTe nanostructures

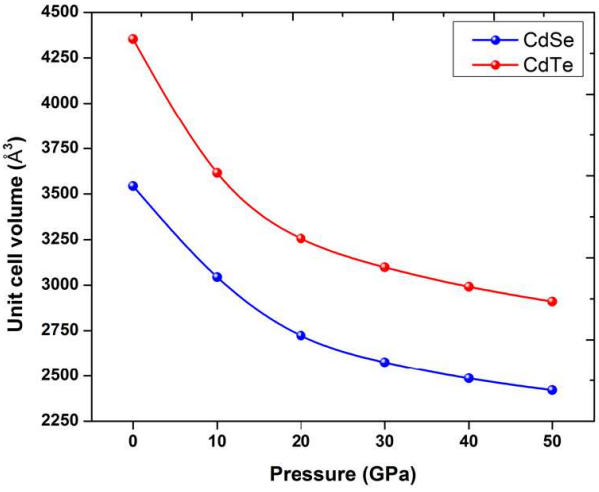

Figure 11. Unit cell volume against uniaxial pressure for CdSe and CdTe nanostructures

luminescent nanowires", *Sci. Adv.*, **3** [5] (2017) 1–8.
9. K. Matsuishi, A. Yuasa, G. Arai, T. Mori, "Structural and optical properties of CdSe nanostructures (nanoparticles, nanoparticle- and nanosheet-superlattices) fabricated using organic molecules as a template", *IOP Conf. Ser. Mater. Sci. Eng.*, **54** (2014) 012007.
10. K. Jacobs, J. Wickham, A.P. Alivisatos, "Threshold size for ambient metastability of rocksalt CdSe nanocrystals", *J. Phys. Chem. B*, **106** [15] (2002) 3759–3762.
11. N.J. Lee, R.K. Kalia, A. Nakano, P. Vashishta, "Pressure-induced structural transformations in cadmium selenide nanorods", *Appl. Phys. Lett.*, **89** [9] (2006) 3–5.
12. C.D. Grant, J.C. Crowhurst, S. Hamel, A.J. Williamson, N. Zaitseva, "Anomalous photoluminescence in CdSe quantum-dot solids at high pressure due to nonuniform stress", *Small*, **4** [6] (2008) 788–794.
13. M.M. Aliyu, M.A. Islam, N.R. Hamzah, M.R. Karim, M.A. Matin, K. Sopian, N. Amin, "Recent developments of flexible CdTe solar cells on metallic substrates: Issues and prospects", *Int. J. Photoenergy*, **2012** (2012) 6–9.
14. T. Seetawan, H. Wattanasarn, "First principle simulation mechanical properties of PbS, PbSe, CdTe and PbTe by molecular dynamics", *Procedia Eng.*, **32** (2012) 609–613.
15. A.M. Martínez, R. Soriano, R. Faccio, A.B. Trigubó, "Mechanical properties calculation of II-VI semiconductors: $Cd_{1-y}Zn_yTe$ ($0 \leq y \leq 1$)", *Procedia Mater. Sci.*, **8** (2015) 656–664.
16. A. Mujica, A. Rubio, A. Muñoz, "High-pressure phases of group-IV, III – V, and II – VI compounds", *Rev. Mod. Phys.*, **75** (2003) 863.
17. M. Côté, O. Zakharov, A. Rubio, M.L. Cohen, "Ab initio calculations of the pressure-induced structural phase transitionsfor four II-VI compounds", *Phys. Rev. B*, **55** [19] (1997) 13025–13031.
18. O. De Melo, C. Vargas-Hernández, I. Hernández-Calderón, "Strain relaxation during the layer by layer growth of cubic CdSe onto ZnSe", *Appl. Phys. Lett.*, **82** [1] (2003) 43–45.
19. J.M. Soler, E. Artacho, J.D. Gale, A. García, J. Junquera, P. Ordejón, D. Sánchez-Portal, "The SIESTA method for ab initio order-N materials simulation", *J. Phys. Condens. Matter*, **14** [11] (2002) 2745–2779.
20. J.P. Perdew, K. Burke, Y. Wang, "Generalized gradient approximation for the exchange-correlation hole of a many-electron system", *Phys. Rev. B*, **54** (1996) [23] 533–539.
21. J. Perdew, J. Chevary, S. Vosko, K. Jackson, M. Pederson, D. Singh, C. Fiolhais, "Atoms, molecules, solids, and surfaces: Applications of the generalized gradient approximation for exchange and correlation", *Phys. Rev. B*, **46** [11] (1992) 6671–6687.
22. R. Bhuvaneswari, R. Chandiramouli, "DFT investigation on the adsorption behavior of dimethyl and trimethyl amine molecules on borophene nanotube", *Chem. Phys. Lett.*, **701** (2018) 34–42.
23. U. Srimathi, V. Nagarajan, R. Chandiramouli, "Interaction of Imuran, Pentasa and Hyoscyamine drugs and solvent effects on graphdiyne nanotube as a drug delivery system - A DFT study", *J. Mol. Liq.*, **265** (2018) 199–207.
24. Y. Le Page, P. Saxe, "Symmetry-general least-squares extraction of elastic data for strained materials from ab initio calculations of stress", *Phys. Rev. B - Condens. Matter Mater. Phys.*, **65** [10] (2002) 1–14.
25. M. Jamal, S. Jalali Asadabadi, I. Ahmad, H.A. Rahnamaye Aliabad, "Elastic constants of cubic crystals", *Comput. Mater. Sci.*, **95** (2014) 592–599.
26. G. Yi, X. Zhang, J. Qin, J. Ning, S. Zhang, M. Ma, R. Liu, "Mechanical, electronic and thermal properties of Cu_5Zr and Cu_5Hf by first-principles calculations", *J. Alloys Compd.*, **640** (2015) 455–461.
27. H. Hu, X. Wu, R. Wang, W. Li, Q. Liu, "Phase stability, mechanical properties and electronic structure of TiAl alloying with W, Mo, Sc and Yb: First-principles study", *J. Alloys Compd.*, **658** (2016) 689–696.
28. S.I. Ranganathan, M. Ostoja-Starzewski, "Universal elastic anisotropy index", *Phys. Rev. Lett.*, **101** [5] (2008) 3–6.
29. N. Kishore, V. Nagarajan, R. Chandiramouli, "High-pressure studies on electronic and mechanical properties of $FeBO_3$ (B = Ti, Mn, Cr) ceramics – A first-principles study", *Phase Transitions*, **1594** (2017) 1–16.
30. H. Ozisik, E. Deligoz, K. Colakoglu, E. Ateser, "The first principles studies of the MgB_7 compound: Hard material", *Intermetallics*, **39** (2013) 84–88.
31. R. Chandiramouli, V. Nagarajan, "First-principles studies on band structure and mechanical properties of $BiFeO_3$ ceramics under high pressure", *Process. Appl. Ceram.*, **11** [2] (2017) 120–126.
32. M. Chauhan, D.C. Gupta, "Electronic, mechanical, phase transition and thermo-physical properties of TiC, ZrC and HfC: High pressure computational study", *Diam. Relat. Mater.*, **40** (2013) 96–106.
33. Y. Tian, B. Xu, Z. Zhao, "Microscopic theory of hardness and design of novel superhard crystals", *Int. J. Refract. Met. Hard Mater.*, **33** (2012) 93–106.
34. S. Dharani, V. Nagarajan, R. Chandiramouli, "Nucleobases adsorption studies on silicane layer: A first-principles investigation", *J. Mol. Graph. Model.*, **85** (2018) 48–55.
35. V. Nagarajan, R. Chandiramouli, "Novel method to detect the lung cancer biomarker volatiles using hydrogen vacant silicane nanosheets: A DFT investigation", *Comput. Theor. Chem.*, **1138** (2018) 107–116.
36. U. Srimathi, V. Nagarajan, R. Chandiramouli, "Adsorption studies of volatile organic compounds on germanene nanotube emitted from banana fruit for quality assessment – A density functional application", *J. Mol. Graph. Model.*, **82** (2018) 129–136.
37. O. Zakharov, A. Rubio, X. Blase, M.L. Cohen, S.G. Louie, "Quasiparticle band structures of six II-VI compounds: ZnS, ZnSe, ZnTe, CdS, CdSe, and CdTe", *Phys. Rev. B Condens. Matter*, **50** [15] (1994) 10780–10787.
38. G. Fonthal, L. Tirado-Mejía, J.I. Marín-Hurtado, H. Ariza-Calderón, J.G. Mendoza-Alvarez, "Temperature dependence of the band gap energy of crystalline CdTe", *J. Phys. Chem. Solids*, **61** [4] (2000) 579–583.